

USING ANTHROPOGENIC WASTE (STEEL SLAG) TO ENHANCE MECHANICAL AND WEAR PROPERTIES OF A COMMERCIAL ALUMINIUM ALLOY A356

The present study addresses the utilization of induction furnace steel slag which is an anthropogenic waste, for enhancing the mechanical properties of a commercial aluminium alloy A356. Different weight percentage (3wt%, 6wt%, 9wt%, and 12wt%) of steel slag particles in 1 to 10 μm size range were used as reinforcing particles in aluminium alloy A356 matrix. The composites were prepared through stir casting technique. The results revealed an improvement in mechanical properties (i.e. microhardness and tensile strength) and wear resistance with an increase in weight percentage of the steel slag particles. This research work shows promising results for the utilization of the steel slag for enhancing the properties of aluminium alloy A356 at no additional cost while assisting at same time in alleviating land pollution.

Keywords: A356, Steel slag, Wear resistance, Tensile strength, Industrial waste, environmental hazard

1. Introduction

Aluminium alloy A356 is one of the most extensively used cast aluminium alloy which exhibits good combination of hardness, corrosion resistance, strength, fatigue, machinability and wear properties. It is widely used in many applications such as in aircraft, aerospace, automotive brake components and power generation (seal rings). Due to the ever increasing performance requirements during service, efforts are continually made by researchers to enhance the properties of existing materials through compositional control, processing variations and optimizing heat treatments. In recent past, composite technology has emerged as a potential route to enhance the properties of monolithic materials. In the case of aluminium alloy A356 reinforcements such as SiC, alumina, graphite and fly ash in different length scales have been incorporated by using different processing techniques [1-10].

Dwivedi et al. investigated the mechanical properties of aluminium alloy A356 with different weight percentage of SiC particle by electromagnetic stir casting method and observed that by increasing the amount of reinforcement, the hardness, tensile strength and fatigue life of the composite material increased [1]. Mazahery et al. studied the mechanical properties of A356/n-SiC synthesized by compo-casting method. The results showed that the hardness and yield strength of the composite improved significantly [2]. Viswanatha et al. investigated the mechanical properties and the microstructure of aluminium alloy A356 reinforced with SiC and Graphite particles and observed that

the hardness and tensile properties shows significant improvement with an increase in the percentage of SiC particles [3]. Hajizamani et al. investigated the mechanical properties of aluminium alloy A356 reinforced with alumina and nano particles of ZrO_2 . The results showed that by increasing the amount of reinforcement the hardness and tensile strength increased [4]. Jayakumar et al. investigated the properties of Aluminium LM25 alloy reinforced with SiC particles fabricated by centrifugal casting. It was observed that the hardness of the composite increased with an increase in volume fraction of the particles [5]. Nagaralet al. studied the mechanical behavior of Aluminium 6061 alloy reinforced with Al_2O_3 and graphite particles and observed that hardness and tensile strength increased by the addition of Al_2O_3 particles, but when the graphite was added along with Al_2O_3 the hardness and the tensile strength decreased [6]. Dwivedi et al. studied the mechanical behavior of A356/SiC and reported that the hardness and tensile strength improved considerably when electromagnetic stir casting method was used [7]. Xiao-Dong et al. investigated Al 5210 composite containing 0.55% volume fraction (V_f) of SiC_p fabricated using squeeze casting method. They reported that the reduction in particle size enhances the interfacial bonding strength and when the particle size increases more defects are produced, which leads to decrease in the strength of the material [8]. Choi et al. studied the microstructure and mechanical properties of A356/ SiO_2 composites processed by friction stir processing method. They reported the homogeneous distribution of particles in the matrix and enhancement in mechanical properties [9]. Tzamtzis et al. investigated the proper-

* SATHYABAMA INSTITUTE OF SCIENCE AND TECHNOLOGY, DEPARTMENT OF MECHANICAL AND PRODUCTION ENGINEERING, CHENNAI, INDIA

** SATHYABAMA INSTITUTE OF SCIENCE AND TECHNOLOGY, DEPARTMENT OF AUTOMOBILE ENGINEERING CHENNAI, INDIA.

*** NATIONAL UNIVERSITY OF SINGAPORE DEPARTMENT OF MECHANICAL ENGINEERING, SINGAPORE

Corresponding author: bupeshvk@gmail.com

ties of A356/SiC composites synthesized using rheocasting and compo casting process. The results established a homogeneous distribution of particles and improvement in tensile strength [10]. Sridhar Raja et al. investigated impact response of steel slag particles reinforced aluminium alloy A356 metal matrix composites. They observed that there was a reduction in impact strength of the aluminium alloy A356 metal matrix composite when compared with the pristine aluminium alloy A356 [11].

From the literature survey it was observed that several investigations have been carried out on aluminium alloy A356 matrix reinforced with ceramic particles like SiC, Al₂O₃, ZrO₂, fly ash etc. which increases its mechanical properties [12-15]. The use of steel slag as reinforcement was used only to investigate impact properties [11]. Further, the literature indicates that the stir casting technique is widely used to make metal matrix composites, due to its low cost, capability to disperse the reinforcement particles reasonably well in the metallic matrix and industrial scalability [16-20].

The induction furnace steel slag is a byproduct produced during the casting of steels. It is produced during the separation of molten steel from impurities in the induction furnaces. The molten metal contains oxides and silicates that solidifies upon cooling which is removed as slag. A large quantity of the slag is disposed as waste product which ends up as landfill adversely affecting the environment. Hence in this study, induction furnace steel slag, an industrial waste, is chosen as the reinforcement material. In this research, the steel slag was pulverized to micron sized particles using ball mill and added to the aluminium alloy A356. The objective of this study is to utilize the discarded steel slag (SS) as reinforcement to produce aluminium metal matrix composites with superior mechanical properties including wear resistance for target application being automotive brake pads.

2. Materials and methods

Commercially available aluminium alloy A356 was used as matrix material. The chemical composition of aluminium alloy A356, conforming to ASTM B117M standard and the physical properties are shown in Table 1 and Table 2, respectively. The concentration of elements in steel slag is shown in Table 3.

Stir casting was used to fabricate metal matrix composites (MMCs) as it is one of the most cost effective and industrially scalable methods. As-received aluminium alloy A356 was placed in the graphite crucible and melted in a muffle furnace. In order to remove moisture and improve the wettability, the steel slag particles were preheated in the furnace at 300°C for 30 minutes along with Potassium Titanate (K₂TiF₆) [11,14]. Steel slag obtained from induction furnace was crushed and pulverized for 3hrs using a ball mill (SPEX 8000D, Ukraine) to obtain particles in the size range of 1-10 μm. To get a homogeneous distribution of the steel slag particles in the aluminium matrix, the steel slag particles were added slowly while the 750°C hot melt was stirred at a speed of 300 rpm. The composite slurry was subsequently poured into a preheated (200°C) permanent steel mold to obtain

TABLE 1

Chemical composition of Aluminium alloy A356 (wt %)

Element	Si	Fe	Cu	Mn	Mg	Ni	Zn	Ti	Al
Wt %	6.58	0.16	0.06	0.06	0.57	0.01	0.01	0.14	Bal

TABLE 2

Properties of Aluminium alloy A356 [7,21]

Liquidus temperature (°C)	615
Density (g/cm ³)	2.685
Tensile strength (MPa)	128
Elongation (%)	13.3
Impact strength (J)	11.5

TABLE 3

Chemical composition of steel slag (wt %)

Element	Fe	Al	Mg	Si	Mn	Ca	Cr	Ti
Wt %	30.0	8.37	0.32	47.44	9.66	2.45	0.58	0.63

97×96×9.8 mm ingot plates. Composite plates containing different weight percentages of steel slag particles (3wt%, 6wt%, 9wt% and 12wt %) were synthesized under identical conditions [22].

By using Archimedes principle the density of the composite was measured in accordance with ASTM B311-08 standard. The weight of the sample was measured in air (W_a) and after immersing in distilled water medium (W_w). According to the Eq. (1) the actual density was calculated.

$$\rho_a = W_a \rho_w / (W_a - W_w) \quad (1)$$

Where, ρ_a is the actual density, W_a is the mass of the sample in the air, W_w is the mass of the sample in the distilled water and ρ_w is the density of the distilled water [23]. For each composition three readings were obtained using distilled water as the immersion media. An electronic balance with an accuracy of ±0.0001 gm was used to record the weights. The theoretical density was calculated by rule of mixtures.

The microstructural characterization of steel slag particles and their distribution was investigated using De-Winton Inverted Trinocular Optical microscope. The Carl Zeiss-Supra 55 Field-Emission Scanning Electron Microscope (FESEM) was used to carry out fractography.

The Rockwell Micro hardness using L-Scale was measured on polished specimens using Wilson Rockwell Hardness-Series 574. A minor load of 10 kg and major load of 60 kg with 5 s dwell time was used conforming to ASTM E10 standards. The hardness readings were taken at four different locations and the average hardness calculated.

The tensile strengths of the composite materials were determined on flat dog bone shaped specimens of 10 mm thickness and 50 mm gauge length using a hydraulic Universal Testing Machine (UTM) conforming to ASTM-B577M. A minimum of three samples for each composite were tested to ensure the accuracy and consistency of results. Fractography investigation was carried out to determine the mode of failure exhibited by composites.

The wear characteristics of the samples were investigated using dry pin-on-disc method in order to study the weight loss of the specimen due to the effect of load and reinforcement conforming to ASTM G99 standard. Specimen size of 6×6×30 mm was used. The weight loss of the composite material was measured before and after the wear tests. The wear tracks were analyzed using Scanning Electron Microscope (SEM).

3. Results and discussion

A356/SS composites were successfully synthesized using stir casting technique with no evidences of macro structural defects. Table 4 shows the comparison of theoretical and experimental density of the composites. It shows that the theoretical density value is either similar or marginally higher

than experimental density value. Results in Table 4 shows that the theoretical density gradually decreases by ~8.5%, whereas the experimental density, determined by Archimedes Principle decreased by ~8.9%. An increase in amount of slag reduced the density of the composites. This can be attributed to the lower density of steel slag (2.6 g/cm³) when compared to that of aluminium alloy A356 (2.67 g/cm³). The theoretical density of the composite was calculated using Eq. (2). The void fraction of the composites was calculated using Eq. (3).

$$\rho_{Th} = \frac{1}{\frac{W_p}{\rho_p} + \frac{W_m}{\rho_m}} \quad (2)$$

$$\text{Void fraction} = \frac{\rho_{Th} - \rho_{exp}}{\rho_{Th}} \quad (3)$$

Where W_p – Weight of steel slag particle, W_m – Weight of aluminium alloy A356, ρ_m – Density of aluminium alloy A356, ρ_p – Density of steel slag particles

Results in Table 4 revealed that the porosity of all samples remained very low ($\leq 0.8\%$) indicating the suitability of stir casting parameters to fabricate the composites in this study.

Fig. 1 (a) and Fig. 1 (b) shows the microstructure of the aluminium alloy A356 matrix at various magnifications. The microstructure of the aluminium alloy A356 matrix showed α -aluminium solid solution with a eutectic mixture of silicon in the aluminium matrix [24-26, 11]. Fig. 1(c) and Fig. 1(d) shows

TABLE 4

Results of density and porosity measurements

A 356 alloy composites	ρ_{Th} (g/cm ³)	ρ_{exp} (g/cm ³)	Void fraction
Aluminium Alloy A356	2.68	2.67	0.0037
A356+3wt% steel slag	2.57	2.57	0.000
A356+6wt% steel slag	2.493	2.49	0.001
A356+9wt% steel slag	2.47	2.46	0.004
A356+12wt% steel slag	2.45	2.43	0.008

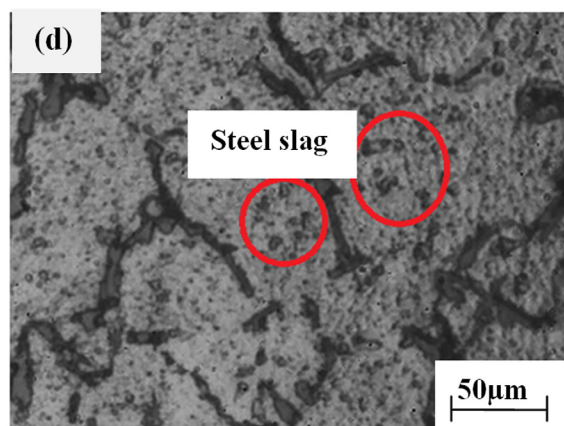
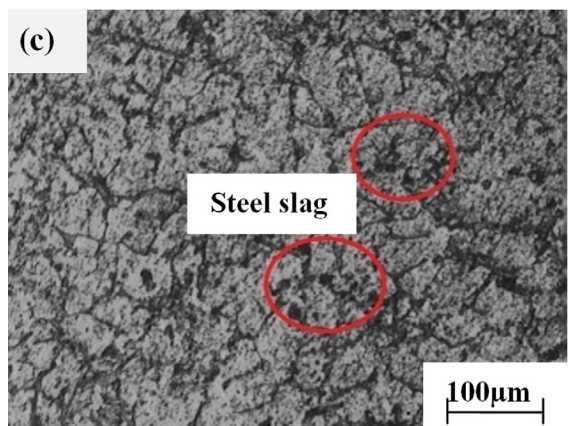
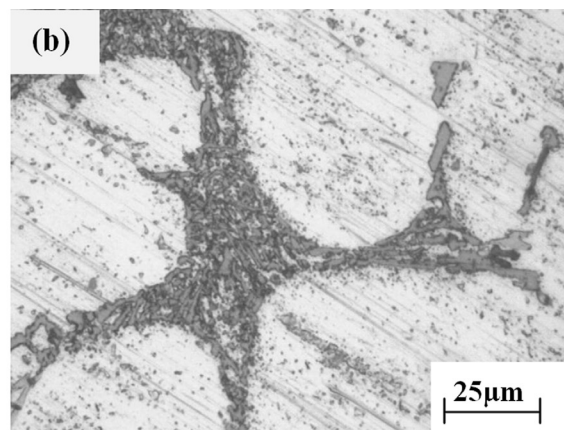
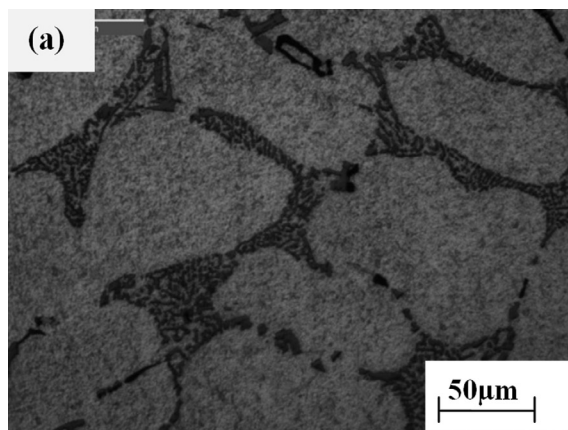


Fig. 1. Optical microstructure of (a) and (b) aluminium alloy A356 matrix (c) and (d) A356/steel slag composite

the A356/steel slag composite exhibiting a relatively homogeneous distribution of steel slag particles. Marked by circle and darker in contrast are steel slag particles present in matrix. Steel slag particles were present mostly along the grain boundaries and some agglomerates were visible in localized areas [27-29]. The detected peaks from EDS analysis correspond to the presence of aluminium, silicon and magnesium which are major constituents of the aluminium alloy A356 and the presence of steel slag particles indicated by the presence of silicon, iron, aluminium, magnesium and other oxides in the material.

The hardness results on monolithic and composite samples are presented in Fig. 2. The results revealed a gradual improvement in hardness with an increase in amount of slag particles in the range of 6-12%. The maximum hardness was about 7.2% higher when compared to aluminium alloy A356 matrix. At 3wt% of slag particles the hardness of the composite was lower than base matrix and indicates that a critical threshold amount of slag particles are required in matrix to realize an improvement in hardness.

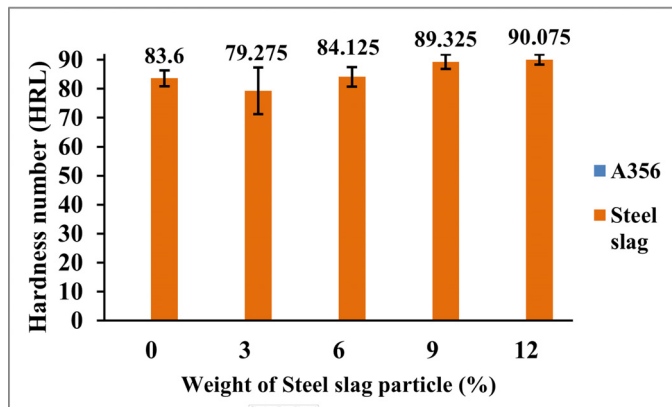
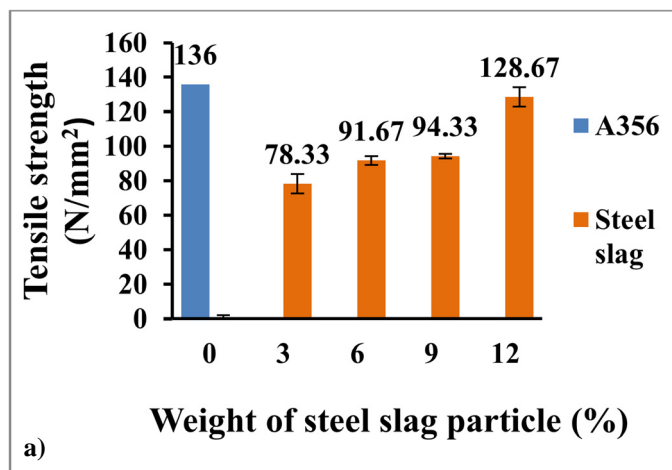


Fig. 2. Hardness of A356/Steel Slag Composites

The results of tensile testing are presented in Fig. 3. From Fig. 3(a) it can be observed that by increasing the weight percentage of the steel slag the tensile strength of the composite increases gradually. Results revealed that strength of monolithic samples



remained superior to composite samples with the strength of composite containing 12wt% reinforcement matches with that of aluminium alloy A356. Within the composites, the strength increased with an increase in amount of slag particles. Results also reveal that an increase in amount of SS particles beyond 12wt% may increase the strength beyond that of aluminium alloy A356. Fig. 3(b) shows that the elongation of all the composite samples remained superior to monolithic aluminium alloy A356 with highest elongation realized for 6wt% steel slag particles containing composite.

Fig. 4 shows scanning electron microscope (SEM) images of tensile fractured samples. Fig. 4(a) corresponds to monolithic material. The fracture surface was flat indicating a brittle fracture that is in conformance to the results of tensile elongation (Fig. 3). For composite samples the fracture surfaces were rough and the presence of isolated near circular voids was observed indicating a ductile-brittle mode of failure. The rough fracture surface suggest an increase in the level of plastic deformation and further indicates that much better strength and elongation can be realized from the composite samples provided these voids can be eliminated by suitably controlling the processing parameters.

The results of wear testing are presented in Fig. 5. The weight loss is reduced in the case of all composite samples with 3wt% composite showing similar weight loss as that of aluminium alloy A356 while 12wt% composite exhibited the minimum weight loss which remains 63% lower when compared to aluminium alloy A356.

Fig. 6 shows the SEM images of the wear tracks in the aluminium alloy A356 matrix and the A356/steel slag metal matrix composite. In Fig. 6(a) the wear tracks are distinctly visible with wear debris spread out on the aluminium alloy A356 matrix. A356/steel slag (3wt%) composite exhibits an extensive wear associated with surface delamination and dislodging of steel slag reinforcing particles from the aluminium alloy A356 matrix. The A356/steel slag (6 and 9wt%) composite shows a reduced wear with few localized wear debris pockets with dislodged reinforcing particles. In Fig. 6(b) A356/steel slag (12wt%) shows very minimal wear debris with shallow wear tracks. This lower debris

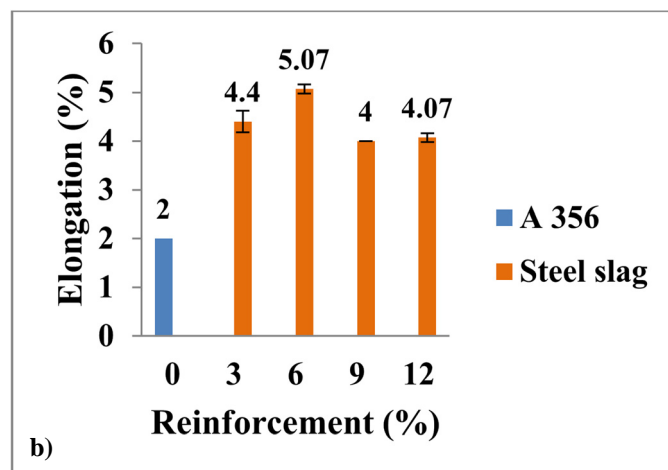


Fig. 3. Results of tensile test of the samples (a) tensile strength (b) elongation

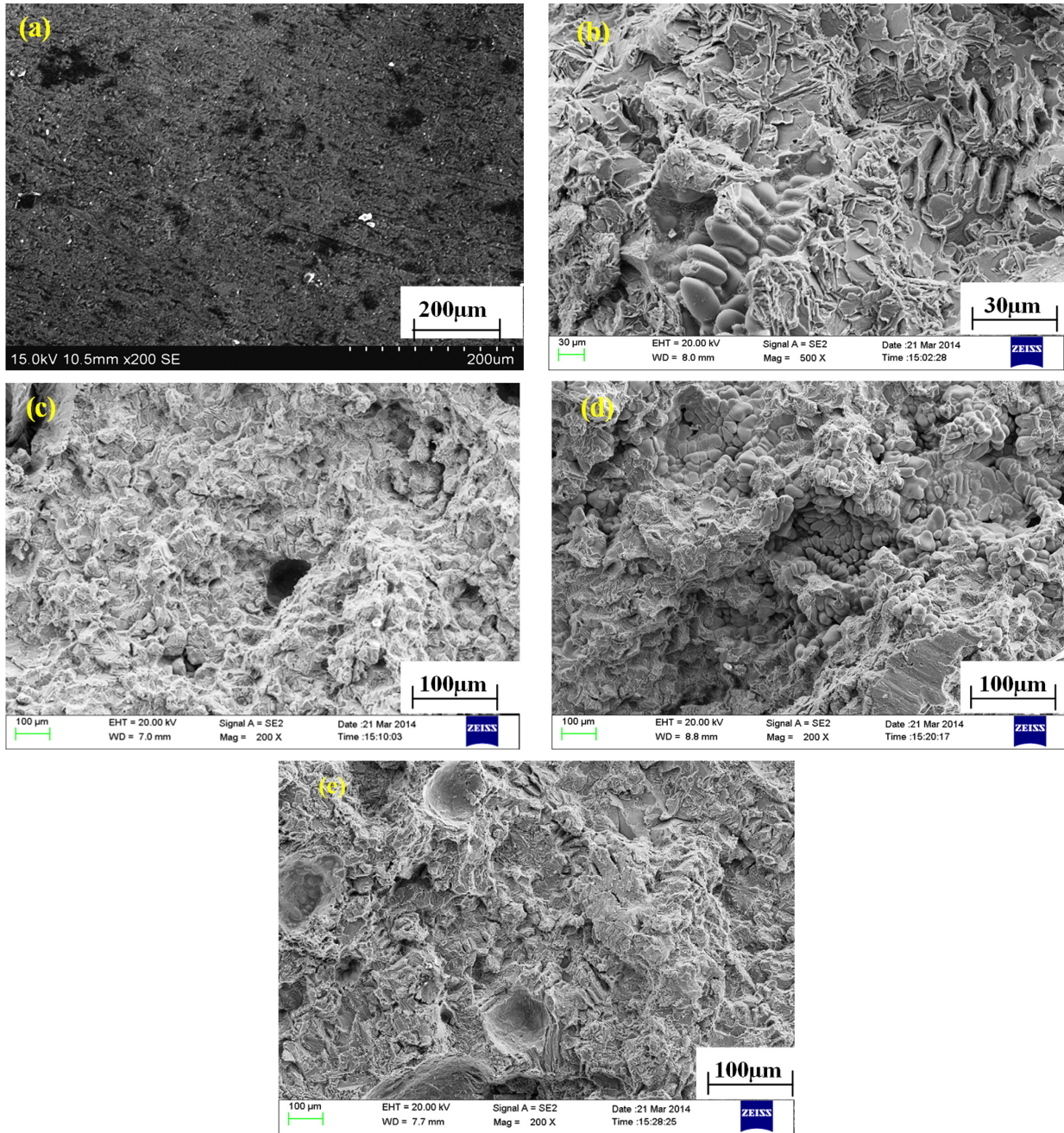


Fig. 4. SEM images of tensile fractured surface: (a) A356 alloy (b) 3wt% of steel slag (c) 6wt% steel slag (d) 9wt% steel slag (e) 12wt% steel slag

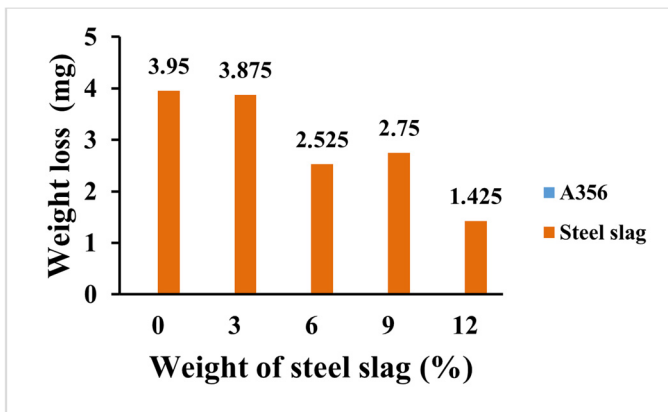


Fig. 5. Wear behavior of monolithic and A356 /steel slag metal matrix composites

indicates good wear resistance and good interface between the particle and the matrix [30].

4. Conclusions

1. Aluminium alloy A356 metal matrix composites containing steel slag particles (upto 12wt%) were fabricated successfully through stir casting technique with minimum porosity.
2. It was observed that increasing the weight percentage of reinforcement, the hardness remains similar (3wt%) or superior (6-12wt%) to monolithic alloy.
3. The tensile strength of the composites remained lower than that of aluminium alloy A356. Composite with 12wt%

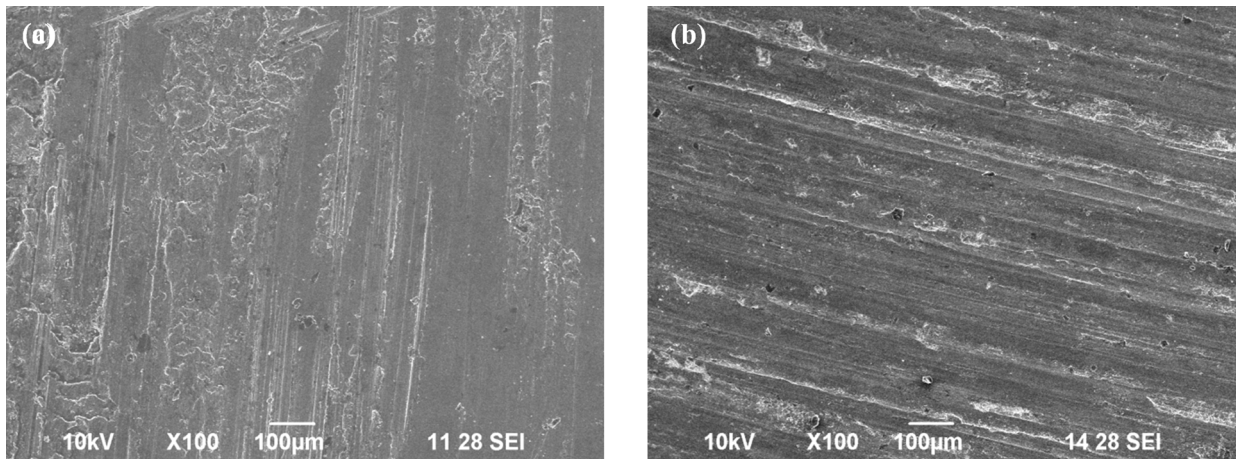


Fig. 6. SEM images of wear tracks: (a) aluminium alloy A356 (b) A356/steel slag composite

reinforcement exhibited similar strength as that of monolithic alloy. Elongation of all composites samples remained superior to monolithic alloy.

4. The wear characteristic shows that by increasing the weight percentage of the steel particles, the weight loss due to wear gets reduced gradually. Also, the wear tracks in SEM images show the amount of debris is lower with an increase in amount of reinforcement.

REFERENCES

- [1] Shashi Prakash Dwivedi, Satpal Sharma, Raghvendra Kumar Mishra, *Procedia Materials Science* **6**, 1524-1532 (2014).
- [2] A. Mazahery, O.M. Shabani, *Strength of materials* **44** (6), 686-692 (2012).
- [3] B.M. Viswanatha, M. Prasanna Kumar, S. Basavara, T.S. Kiran, *Journal of Engineering Science and Technology* **8** (6), 754-763 (2013).
- [4] M. Hajizamani, H. Baharvandi, *Advances in Materials Physics and Chemistry* **1**, 26-30 (2011).
- [5] A. Jayakumar, M. Rangaraj, *International Journal of Emerging Technology and Advanced Engineering* **4** (2), 495-501 (2014).
- [6] M. Nagaral, V. Auradi, M.K. Ravishankar, *International Journal of Research in Engineering and Technology* **1** (2), 193-198 (2013).
- [7] Shashi Prakash Dwivedi, Satpal Sharma, Raghvendra Kumar Mishra, *International Journal of Manufacturing Engineering* 1-13 (2014).
- [8] Y.U. Xiao-Dong, W. Yang-Wei, W. Fu-chi, *Transactions of Non-ferrous Metals Society of China* **17**, 276-279 (2007).
- [9] Don-Hyun Cho, Yong-Hwan Kim, Byung-Wook Ahn, Yong-Il Kim, Seung-Boo Jung, *Transactions of Nonferrous Metals Society of China* **23**, 335-340 (2013).
- [10] S. Tzamtzis, N.S. Barekar, N. Hari Babu, J. Patel, B.K. Dhindaw, Z. Fan, *Composites: Part A* **40**, 144-15 (2009).
- [11] K.S. Sridhar Raja, V.K. Bupesh Raja, K.R. Vignesh, S.N. Ramana Rao, *Applied Mechanics and Materials* **766-767**, 240-245 (2015).
- [12] J. Bienia, M. Walczak, B. Surowska, B.J. Sobczaka, *Journal of Optoelectronics and Advanced Materials* **5** (2), 493-502 (2003).
- [13] K.K. Alaneme, P.A. Olubambi, *Journal of Materials Research and Technology* **2** (2), 188-194 (2013).
- [14] D.S. Prasad, C.S. hoba, *Journal of Materials Research and Technology* **3** (2), 172-178 (2014).
- [15] K. Kanayo Alaneme, K. Oladiti Sanusi, *Engineering Science and Technology an International Journal* **18**, 416-422 (2015).
- [16] K.R. Ravi, V.M. Sreekumar, R.M. Pillai, M. Chandan, K.R. Amaranathan, K.R. Arul, *Materials & Design* **28**, 871-881 (2007).
- [17] K.B. Shorowordi, T. Laoui, A.S.M.A. Haseeb, J.P. Celis, L. Froyen, *Journal of Materials Processing Technology* **142**, 738-743 (2003).
- [18] I. Kerti, F. Toptan, *Materials Letters* **62**, 1215-1218 (2008).
- [19] A. Mortensen, National Laboratory, Roskilde, Denmark. 141 (1998).
- [20] B.C. Pai, K.G. Sathyanarayana, P. Robi, *Journal of Materials Science Letters* **11**, 779-781 (1992).
- [21] H. Shueiwan, J. Shyh-Ming Wu, *Journal of Marine Science and Technology* **16** (4), 271-274 (2008).
- [22] K.S. Sridhar Raja, V.K. Bupesh Raja, *International Journal on Design and Manufacturing Technologies* **7**, 29-32 (2013).
- [23] H.M. Zakaria, Ain Shams, *Engineering Journal* **5**, 831-838 (2014).
- [24] K. Haider, Md. Azad Alam, A. Redhewal, V. Saxena, *International Journal of Engineering Research and Applications* **5**, 63-69 (2015).
- [25] S.P. Dwivedi, A. Srivastava, A. Kumar, B. Nanda, *Indian Journal of Engineering and Materials Sciences* **24**, 133-140 (2017).
- [26] D. Siva Prasad, Ch. Shoba, N. Ramanaiah, *Journal of Materials Research and Technology* **70**, 1-7 (2017).
- [27] R. Brown, (Ed), *Foseco, Non-Ferrous foundryman's handbook*. In *Butterworth-Heinemann Aluminium casting alloys*, Elsevier (1999).
- [28] S. Salem, T. Sjogren, L. Svensson, *Metallurgical Science and Technology* **25** (1), 12-22 (2007).
- [29] L. Backerud, G. Chai, J. Tamminen, (Ed.2), *Solidification characteristics of aluminium alloys*, *Foundry alloys 2 AFS/SKANALUMINIUM* (1990).
- [30] T.C. Tszeng, *Composites* **B29B**, 299-308 (1998).
- [31] S. Ahmed, F.R. Jones, *Composites* **21**, 81-84 (1990).
- [32] J. Subramanian, Z. Loh, S. Seetharaman, A. S. Hamouda, M. Gupta, *Metals* **2**, 178-197 (2012).
- [33] K.R. Suresh, H.B. Niranjana, P. Martin Jebaraj, M.P. Chowdiah, *Wear* **255**, 638-642 (2003).